Iterative Multiuser Decoding with an Unknown Number of Users: Large-System Analysis

A. Tauste Campo and A. Guillén i Fàbregas

CUED / F-INFENG / TR 622
January 2009

Iterative Multiuser Decoding with an Unknown Number of Users: Large-System Analysis

Adrià Tauste Campo and Albert Guillén i Fàbregas

Abstract

We study iterative multiuser detection in large randomly spread code division multiple access systems under the assumption that the number of users accessing the channel is unknown by the receiver. In particular, we focus on the factor graph representation and iterative algorithms based on belief propagation. We build an iterative scheme that detects the encoded data and the users' activity. By using the replica method from statistical physics, we characterize the density evolution of the iterative detector when the number of potential users is large. As a result, we provide a general fixed-point equation where the nature of the exchanging probabilities depends on to the users' activity. Finally, we show that the structure of the users' codes yields a multiuser efficiency fixed-point equation that is equivalent to the case of all-active users with a system load scaled by the activity rate.

A. Tauste Campo and A. Guillén i Fàbregas are with the Department of Engineering, University of Cambridge, Trumpington Street, Cambridge CB2 1PZ, UK, e-mail: `at461@cam.ac.uk, albert.guillen@eng.cam.ac.uk`.

I. INTRODUCTION

The interplay between multiuser detection (MUD) and channel coding in multiple-access channels has been recently studied from different angles. From an information-theoretic perspective, the capacity region of the Gaussian multiple-access channel is known to be achievable by successive interference cancellation (IC) and single-user decoding [1]. Practical approaches based on code division multiple access (CDMA) and iterative joint decoding have also been studied [2], [3], [4], [5].

In [4], the authors provide a unified framework to analyze the performance of iterative multiuser joint decoding with CDMA in the limit for large block length and system dimensions. Their approach is based on a factor graph representation of the probability mass function (p.m.f.) of the system using the belief propagation or sum-product algorithm [6] to estimate it. This characterization allows the derivation of iterative algorithms that approximate optimal maximum a posteriori (MAP) decoding. The asymptotic performance of belief propagation can be analyzed by using *density evolution* techniques [7]. Based on results from linear MUD for uncoded systems [8] and [4] characterized the performance of large multiuser systems using suboptimal iterative IC and decoding with linear filtering.

Similarly, using the key result for the large-system analysis of optimal MUD for uncoded systems [9], the authors in [5] use the replica method to characterize the large-system performance of the belief propagation iterative joint decoder. In contrast with previous work on uncoded CDMA [10], [11], the system performance is now determined by the stable fixed-points of a mapping based on density evolution. Since the decoder extrinsic messages are approximated as a posteriori probabilities (APP's) of an equivalent Gaussian channel, density evolution with a Gaussian approximation (DE-GA) can be described by a one-dimensional dynamical system.

In this paper, we present a general treatment of large-system analysis of iterative multiuser joint adopting the approach of [12], in which the number of users accessing the channel is variable and must be estimated together with the transmitted data. We derive the new fixed-point equations to the corresponding density evolution algorithm. In order to derive the these fixed-point equations we use the large-system analysis presented in [13].

This paper is organized as follows. Section II introduces the system model and the main notations used throughout. Section III describes the iterative MUD factor graph and the belief propagation decoding algorithm. Section IV presents the main results on density evolution and Gaussian approximation, showing the corresponding generalized dynamic fixed-point equations. Finally, section VI draws some concluding remarks. Proofs can be found in the appendices.

II. SYSTEM MODEL

We consider a synchronous Gaussian CDMA system where K is the maximum number of users entitled to access the system, N is the length of the spreading sequences and L is the length of the users' codewords. The corresponding received signal matrix is given by

$$\boldsymbol{Y} = \boldsymbol{S}\boldsymbol{A}\boldsymbol{X} + \boldsymbol{Z} \tag{1}$$

where $\boldsymbol{Y} \in \mathbb{R}^{N\times L}$ is the received signal, $\boldsymbol{S} \in \mathbb{R}^{N\times K}$ is the matrix of the spreading sequences, $\boldsymbol{A} = \mathrm{diag}(a_1, \dots, a_K) \in \mathbb{R}^{K\times K}$ is the diagonal matrix of the users' signal amplitudes, $\boldsymbol{Z} \in \mathbb{R}^{N\times L}$ is an additive white Gaussian noise matrix with i.i.d. entries $\sim \mathcal{N}(0, \frac{1}{2})$, and $\boldsymbol{X} = (\boldsymbol{x}_1, \dots, \boldsymbol{x}_K)^{\mathsf{T}} \in \mathbb{R}^{K\times L}$ is the matrix containing the users' coded blocks, where $\boldsymbol{x}_k = (x_{k,1}, \dots, x_{k,L})^{\mathsf{T}}$.

We assume that users are active with probability $\alpha \triangleq \Pr\{\text{user } k \text{ active}\}$, $1 \le k \le K$. We assume that active users employ binary-shift keying (BPSK) modulation with equal probabilities. Hence, each component $x_{k,l}$ of $\boldsymbol{x}_k$ belongs to a ternary constellation $\mathcal{X} \triangleq \{-1, 0, +1\}$ with prior probabilities $\Pr\{x_{k,l} = -1\} = \Pr\{x_{k,l} = +1\} = \frac{\alpha}{2}$ and $\Pr\{x_{k,l} = 0\} = 1 - \alpha$. We also assume that $a_k = \sqrt{\gamma}$, where γ is the average received signal-to-noise ratio (SNR)[1].We define the maximum system load as $\beta \triangleq \frac{K}{N}$.

[1]The analysis presented in this paper can be easily extended to different statistics of the a_k coefficients, like for example those induced by Rayleigh fading.

A. Encoding of data and activity

Let $\boldsymbol{B} = (\boldsymbol{b}_1, \ldots, \boldsymbol{b}_K)^\mathsf{T} \in \mathbb{R}^{K\times B}$ be the information bit matrix of all users, where B is the length of an information message and $\boldsymbol{b}_k = (b_{k,1}, \ldots, b_{k,B})^\mathsf{T}$. Whenever user k is active, then $\boldsymbol{b}_k \in \mathbb{F}_2^B$, otherwise $\boldsymbol{b}_k = (2, \ldots, 2)$. We assume that active-user vectors are encoded independently with probability α and the inactive message appears with probability $1-\alpha$. The nature of the information messages varies significantly from active to inactive users. For instance, it is easy to see that in the case of inactive users, the information symbols are not independent: if the first one is represented by 2, all the rest are 2 as well. In order to incorporate the activity of users into the decoding process, we add one pilot symbol at the beginning of each coded block, which can be either one or zero, depending on whether the user is active or not, respectively. Hence, if user k is active, we can define an encoding function $\phi_k : \mathcal{M}_k \to \{-1, +1\}^L$ such that

$$\phi_k(m_k) = (x_{k,1}, \ldots, x_{k,L}) \in \mathcal{C}_k \tag{2}$$

and the code $\mathcal{C}_k$ is then defined as:

$$\mathcal{C}_k = \{\boldsymbol{x} \in \{-1, +1\}^L : \boldsymbol{x} = (+1, \phi_k(m_k)), \quad \forall m_k \in \mathcal{M}_k\} \tag{3}$$

where $\mathcal{M}_k$ the message set. If the user is inactive, the user code $\mathcal{C}_k$ is only modulated as follows:

$$\mathcal{C}_k = \{\boldsymbol{x} = (0, \ldots, 0)\}. \tag{4}$$

Note that this is equivalent to considering a code $\tilde{\mathcal{C}}_k$ that incorporates the all-zero modulated codeword representing the non-activity. While the presentation given in this paper is general, we will focus our examples on trellis codes. The coded BPSK streams are first interleaved across time (Π_1), and once the activity comes into play, they are interleaved across user dimensions (Π_2), so that the resulting vectors accessing the channel are independent. This corresponds to a system with coordinated but non-cooperative users, where information is available at a common point. The interleaved signals are then spread and transmitted over the channel. The system is depicted in Fig. 1, where one can observe the encoding/decoding block, the random interleaver/deinterleaver and the optimum detector.

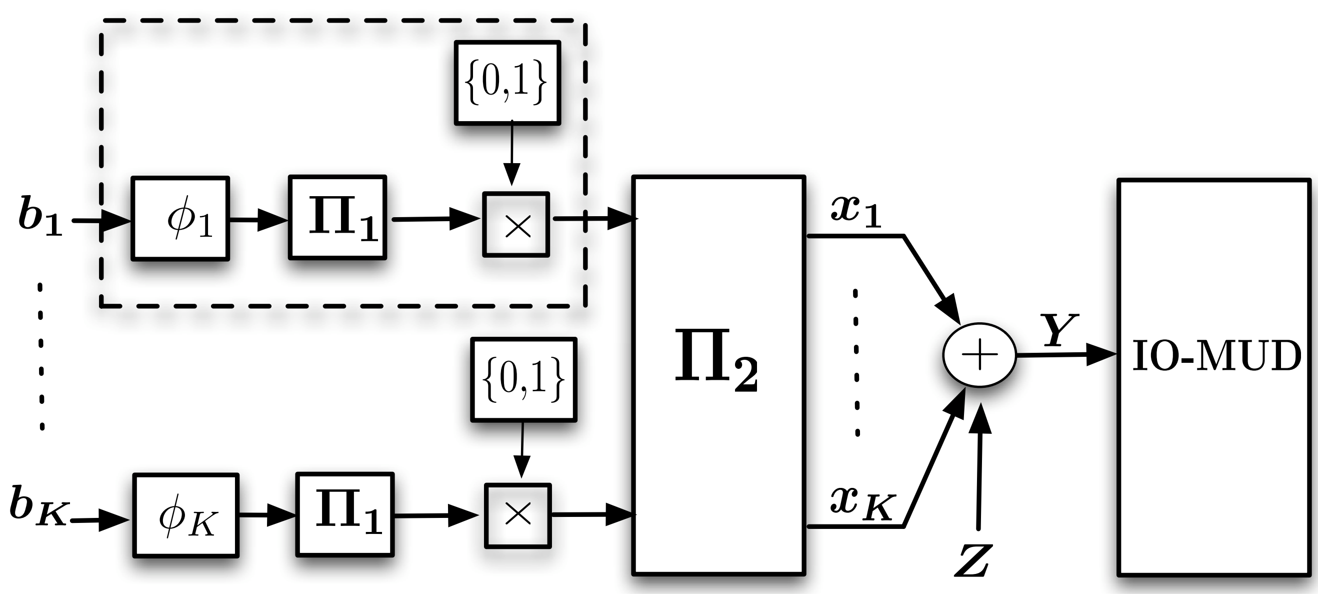

Fig. 1. Block diagram of the proposed multiuser system

When the underlying users' codes are convolutional, the above considerations result in a trellis that combines the activity and encoding functions. This is shown in Fig. 2 for the first stages of a convolutional code $(5,7)_8$. We represent the inactivity with the upper all-zero branch, while users' activity corresponds to the lower branch that contains the code structure. In particular, when the codes are trellis codes, the overall trellis can be decoded with the forward-backward algorithm [14]. The two graphs are linked in the initial state S_0 and become independent after the arrival of the pilot symbol. Note that the upper branch corresponds to a repetition code of rate $1/L$.

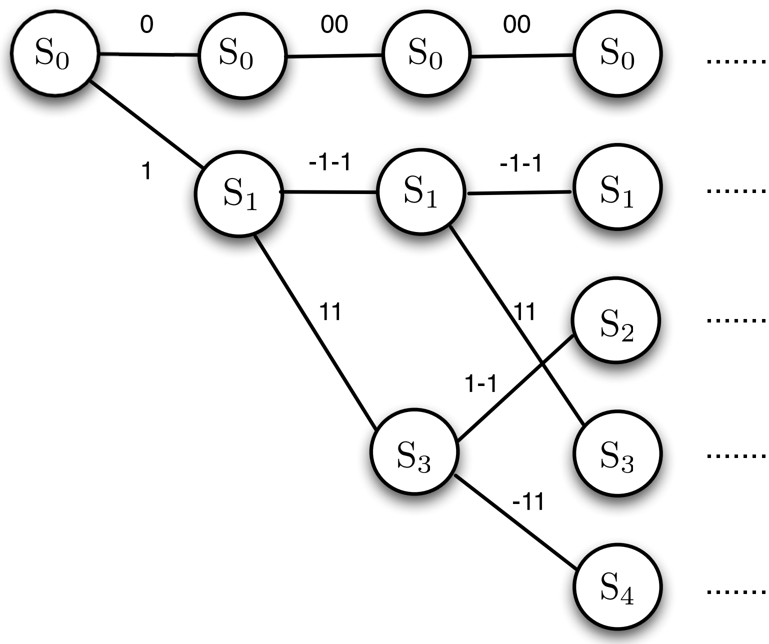

Fig. 2. Modified trellis structure of a convolutional code $(5,7)_8$.

B. Optimum detection

Assuming that the receiver knows $\boldsymbol{S}$ and $\boldsymbol{A}$, the a posteriori probability (APP) of the transmitted data has the form

$$p(\boldsymbol{X}|\boldsymbol{Y},\boldsymbol{S},\boldsymbol{A}) = \frac{1}{\sqrt{\pi}} e^{-\|\boldsymbol{Y}-\boldsymbol{S}\boldsymbol{A}\boldsymbol{X}\|^2} \frac{p(\boldsymbol{X})}{p(\boldsymbol{Y}|\boldsymbol{S},\boldsymbol{A})}. \tag{5}$$

Hence, the maximum a posteriori (MAP) joint activity-and- data multiuser detector solves

$$\hat{\boldsymbol{X}} = \arg \max_{\boldsymbol{x}\in\mathcal{X}^{K\times L}} p(\boldsymbol{X}|\boldsymbol{Y},\boldsymbol{S},\boldsymbol{A}). \tag{6}$$

Similarly, optimum detection of single-user data and activity is obtained by marginalizing over the undesired users as follows:

$$\hat{\boldsymbol{x}}_k = \arg\max_{\boldsymbol{x}_k} \sum_{\boldsymbol{X}\in\{\mathcal{X}^{K\times L}\setminus\boldsymbol{x}_k\}} p(\boldsymbol{X}|\boldsymbol{Y},\boldsymbol{S},\boldsymbol{A}). \tag{7}$$

Although $\boldsymbol{x}_k$ does not necessarily correspond to the k-th user's codeword due to the interleaver, the interleaver is a bijective map, and allows to recover a particular user's signal by appropriate de-interleaving.

III. Iterative joint decoding: Factor graph and belief propagation

We recall the canonical factor graph representation of a multiuser coded system [4] in order to compute the a posteriori p.m.f. of the information symbols:

$$\Pr(\boldsymbol{b}_1, \ldots, \boldsymbol{b}_K | \boldsymbol{y}, \boldsymbol{S}, \boldsymbol{A}) \tag{8}$$

The computation of (8) by brute force is infeasible even for small maximum number of users. We consider the application of the well-known sum-product algorithm to the aforementioned factor graph [6]. In particular, we focus on the belief propagation method, which iteratively approximates the marginal probabilities of (8). This approximation is carried out trough message passing between the optimum multiuser detector (IO-MUD) and the users' soft-input soft-output (SISO) decoders.

We denote the outgoing messages from the IO-MUD at iteration $\ell \in \mathbb{N}$, for signal $k = 1, \ldots, K$ and time $l = 1, \ldots, L$ as $\boldsymbol{q}_{k,l}^{(\ell)} = \left(q_{k,l}^{(\ell)}(-1), q_{k,l}^{(\ell)}(0), q_{k,l}^{(\ell)}(1)\right)$. The outgoing messages from the SISO decoder are denoted as $\boldsymbol{p}_{k,l}^{(\ell)} = \left(p_{k,l}^{(\ell)}(-1), p_{k,l}^{(\ell)}(0), p_{k,l}^{(\ell)}(1)\right)$, and are the extrinsic probabilities of the coded symbols. When the users' codes are convolutional codes, the messages $\boldsymbol{p}_{k,l}^{(\ell)}$ are obtained by applying the forward-backward algorithm to the combined trellis.

According to [6], [4], the general sum-product rules that relate both sets or probabilities are stated as follows:

$$q_{k,l}^{(\ell)}(x) \propto \sum_{\boldsymbol{x} \in \mathcal{A}_1 \times \cdots \times \mathcal{A}_K, x_{k,l} = x} \exp\left(-\left|\boldsymbol{y}_l - \sum_{j=1}^{K} \boldsymbol{s}_j a_j x_{j,l}\right|^2\right) \prod_{j \neq k} p_{j,l}^{(\ell-1)}(x_{j,l}), \quad \text{for } x \in \mathcal{A}_k \tag{9}$$

$$p_{k,l}^{(\ell+1)}(x) \propto \sum_{\{\boldsymbol{x} \in \mathcal{C}_k, x_{k,l} = x\}} \prod_{j \neq l} q_{k,j}^{(\ell)}(x) \tag{10}$$

We assume that the messages $\boldsymbol{p}_{k,l}^{(0)} = (\frac{\alpha}{2}, 1-\alpha, \frac{\alpha}{2})$ for $k = 1, \ldots, K$ and time $l = 1, \ldots, L$. Note that the above messages can be viewed as random variables, which depend on both the channel and code parameters.

Finally, the approximation of the APP of any information symbol b by means of belief propagation is given by:

$$\mathrm{APP}_{k,l}^{(\ell)}(b) \propto \sum_{\boldsymbol{x} = \phi_k(\boldsymbol{b}), b_{k,l} = b} \prod_{j=1}^{L} q_{k,j}^{(\ell)}(x_{k,j}) \tag{11}$$

IV. Density evolution

In order to characterize the performance over the iterations, we are interested in studying the evolution of the p.d.f. of the above messages. This can be done by means of a procedure named *density evolution*. Density evolution has been applied to study iteratively decoded codes such as turbo and low-density parity check (LDPC) codes [7] as well as iterative MUD [4], [5]. Density evolution is based on the principle that as the length of the code is sufficiently large, the p.d.f. of the messages becomes deterministic. In this section, we study density evolution for our MUD problem with an unknown number of users. In particular, we study the large-system limit, i.e., when the number of users and the spreading sequence dimension grow large, but their ratio is kept fixed. We employ statistical physics techniques to characterize the nature of the messages $\boldsymbol{q}_{k,l}^{\ell}$.

A. Concentration

The concentration theorem in [4] for the coded CDMA channel model under some conditions on the user codes $\mathcal{C}_k$ refers to the existence of a limiting distribution of the output messages $\boldsymbol{p}_{k,l}^{(\ell)}$ for $L \to \infty$. In order to validate the concentration result in our particular system, recall the way the inactivity was characterized as a rate $1/L$ repetition code. Then, the probability of making a correct decision on the activity is given by the following result.

Proposition 4.1: The success probability P_s of a repetition code of rate $1/L$ satisfies

$$P_s = 1 - \left(2Q\left(\frac{\sqrt{\eta\gamma}}{2}\right)\right)^{L/2+1}. \tag{12}$$

Under the assumptions of density evolution, i.e., $L \to \infty$, the success probability $P_s \to 1$. This implies that the activity detection will always be perfect in the iterative process in the limit for large codeword length. We therefore consider a compound of two types of message probabilities that switch depending on whether soft decoding operates on an active or an inactive coded block. We thus assume that according to Proposition 4.1, we have perfect activity detection. Consequently the limiting distribution of the messages over an active block exists under the same conditions as in the general case [4], whereas the limiting distribution of the messages over an inactive one concentrates all the probability in the inactivity symbol.

B. Large-System Analysis

The concentration theorem is valid for $L \to \infty$ but finite K and N. However, the analysis with finite K and N can be complicated. On the other hand, large-system analysis is remarkably simpler and accurately mimics the behavior of the system for not-so-large dimensions. In particular, we let $K, N \to \infty$ keeping their ratio, the system load $\beta = K/N$, fixed. Under these conditions [4], we invoke the decoupling principle [10], [13] for optimum MUD, and use its single-user characterization. The result has the following original form:

Claim 4.2 ([13]): In the large-system limit, the distribution of the output of the individually optimal detector of the multiuser channel conditioned on $X_k = x$, converges to the distribution of a posterior mean estimate of a single-user Gaussian channel conditioned on $X = x$ being transmitted.

In other words, the marginal probabilities computed at the IO-MUD can be regarded as the output of an equivalent Gaussian channel where the noise is distributed as $\mathcal{N}(0, 1/(\gamma_k \eta^{(\ell)}))$, where $\eta^{(\ell)}$ is the multiuser efficiency at iteration ℓ. The multiuser efficiency characterizes the degradation factor of the SNR due to the multiple-access interference. The multiuser efficiency minimizes the free energy [9]

$$\mathcal{F} = \frac{1}{K} \log\left(p(\boldsymbol{y})\right) \tag{13}$$

and it is called the globally stable solution of the system.

We now present our main results on dynamical system behavior that updates the distribution of the IO-MUD messages at each iteration. Our approach is more general than previous work and takes into account the fact that the distribution of the SISO message depends on the users' activity. Note that due to the large-system approach, the the extrinsic probabilities outgoing from the SISO decoders $\boldsymbol{p}_{k,l}^{(\ell)}$ are independent of k and l. To simplify the notation we denote the extrinsic probabilities by $\boldsymbol{p}_{\text{ext}}^{(\ell)}$. We assume equal power for each users and we omit the subscript k in the SNR. The updating parameter, $\eta^{(\ell)}$, is given in terms of a one-dimensional fixed-point equation $\eta^{(\ell)} = \Psi(\eta^{(\ell-1)}, \beta, \alpha, \gamma)$, which is derived using the replica method.

Claim 4.3: Consider a general iterative MUD system where the number of users is unknown and parameterized by a Bernoulli variable A_α with success probability α. Then, the multiuser efficiency at iteration ℓ of a BP iterative joint multiuser decoder is given by the globally stable solution of the following fixed point equation:

$$\eta^{(\ell)} = \left(1 + \beta \mathbb{E}_{A_\alpha, \boldsymbol{p}_{\text{ext}}^{(\ell-1)}, Y, X, \gamma}\left[\gamma\left(X - \hat{X}(\eta^{(\ell-1)}, \eta^{(\ell)}, \gamma)\right)^2\right]\right)^{-1} \tag{14}$$

where $\hat{X}(\eta^{(\ell-1)}, \eta^{(\ell)}, \gamma) = \mathbb{E}[X|Y, \gamma]$ is the MMSE estimate.

The general result given in Claim 4.3 can be easily applied to our system, where the activity is perfectly detected after the first iteration for arbitrary SNR and $L \to \infty$. We have the following result.

Corollary 4.4: The fixed-point equation of a system with unknown number of equal-power users that perfectly estimates their activity at a particular iteration $\eta^{(\ell-1)} > 0$ converges with probability 1 to:

$$\eta^{(\ell)} = \left(1 + \beta'\gamma\left(1 - \mathbb{E}_{\boldsymbol{p}_{\text{ext}},Y,X,\gamma|A_\alpha=1}\left[\gamma\hat{X}^2(\eta^{(\ell-1)}, \eta^{(\ell)}, \gamma)\right]\right)\right)^{-1} \tag{15}$$

where $\beta' = \beta\alpha$ and $\hat{X}(\eta^{(\ell-1)}, \eta^{(\ell)}, \gamma) = \mathbb{E}[X|Y, \gamma]$ is the MMSE estimate.

Note that the above result is exactly the fixed-point equation of a system with a fixed (and known) number of users with load $\beta' = \beta\alpha$ for any $\eta^{(\ell-1)} > 0$. In the case of $\eta^{(\ell-1)} = 0$, the result does not hold as it corresponds to the uncoded case [15]. The above fixed-point equation can be further developed by using strictly some approximations of the extrinsic probabilities when an active block is transmitted.

C. Approximations

Based on common empirical observations, we can approximate the outgoing message from the SISO decoder as the output of a virtual equivalent Gaussian channel where the noise is modeled as $\mathcal{N}(0, 1/(\mu^{(\ell)}))$. The approximation allows some degrees of freedom in the choice of μ. As in [5], we choose the following matching

$$\mu^{(\ell)} = Q^{-1}\left(P_e(\gamma\eta^{(\ell)})\right) \tag{16}$$

where $P_e(\rho)$ is the symbol error probability where decisions are made from extrinsic probabilities of the SISO decoders for a general input with SNR ρ. This characteristic can be obtained by simple simulation over the AWGN channel, or a combination of simulation and bounding techniques [4].

By the above Gaussian approximation we can recover the dual result of [5]:

Corollary 4.5: Assume the Gaussian approximation postulated above for the SISO decoders. Then, the fixed-point equation for $\ell > 1$ converges with probability 1 to

$$\eta^{(\ell)} = \left[1 + \beta'\gamma\left(1 - \int_{\mathbb{R}^2} \frac{1}{2\pi} e^{-\frac{(y^2+z^2)}{2}} \tanh\left(\eta^{(\ell)}\gamma + \mu(\eta^{(\ell-1)}\gamma) - \sqrt{\eta^{(\ell)}\gamma}y - \sqrt{\mu(\eta^{(\ell-1)}\gamma)}z\right)\mathrm{d}y\mathrm{d}z\right)\right]^{-1} \tag{17}$$

where $\beta' = \beta\alpha$.

In the large SNR regime, the MMSE

$$\text{MMSE} = 1 - \int_{\mathbb{R}^2} \frac{1}{2\pi} e^{-\frac{(y^2+z^2)}{2}} \tanh\left(\eta^{(\ell)}\gamma + \mu(\eta^{(\ell-1)}\gamma) - \sqrt{\eta^{(\ell)}\gamma}y - \sqrt{\mu(\eta^{(\ell-1)}\gamma)}z\right)\mathrm{d}y\mathrm{d}z \tag{18}$$

admits a somewhat simpler form, which results in a simpler expression for the fixed point equation (17). As shown in [15], large-SNR analysis of the MMSE leads to interesting results for high quality-of-service applications. However, in this case, the dependence of the asymptotic MMSE on the system parameters is less straightforward as in the uncoded case, as illustrated by the following result.

Proposition 4.6: The large system MMSE for an iterative multiuser joint detector with SNR γ and multiuser efficiency η using the SISO decoder Gaussian approximation described by $\mathcal{N}(0, \frac{1}{\mu(\eta\gamma)})$ is given in the high-SNR regime by

$$\lim_{\gamma\to\infty} \text{MMSE} = \sqrt{\frac{2}{\pi}} \frac{e^{-\frac{\eta\gamma}{2} - \mu(\eta\gamma) - \frac{\kappa_1^2}{2} + \frac{(1+\kappa_1)\sqrt{\mu}}{2(1+\kappa_2)}}}{\sqrt{\eta\gamma} + \kappa_1\left(1 - \frac{(1+\kappa_1)}{(1+\kappa_2)^2}\right)} \tag{19}$$

where $\kappa_1 \triangleq \frac{\mu(\eta\gamma)}{\sqrt{\eta\gamma}}$ and $\kappa_2 \triangleq \frac{\mu(\eta\gamma)}{\eta\gamma}$.

V. Numerical results

The above results imply that the analysis of a coded multiuser system with user-and-data detection can be easily converted into the analysis of a standard multiuser system where the number of users is fixed and known. By using the trellis structure introduced in Section II, the activity is detected perfectly with one iteration, and the behavior of the dynamical fixed-point equation has the form of a data detector with a scaled system load.

In Fig. 3 we show the density evolution mapping function for the standard case ($\alpha = 1$) and an example of a case where all users are not active ($\alpha = 0.5$) using the above Gaussian approximation. It can be seen that this approximation (solid line) matches well the actual system behavior (dashed line). On the other hand, a symmetric Gaussian approximation (classical approximation) for each extrinsic symbol does not match well the system behavior (dash-dotted line). Remark that the standard case with $\alpha = 1$ finds a fixed point that at very low multiuser efficiency. On the contrary, when all users are active with probability $\alpha = 0.5$, this point is avoided and the unique solution is $\eta = 1$. Hence, the activity rate works as a scaling factor of the system load and avoids fixed points at low iterations which usually represent very low values of multiuser efficiency.

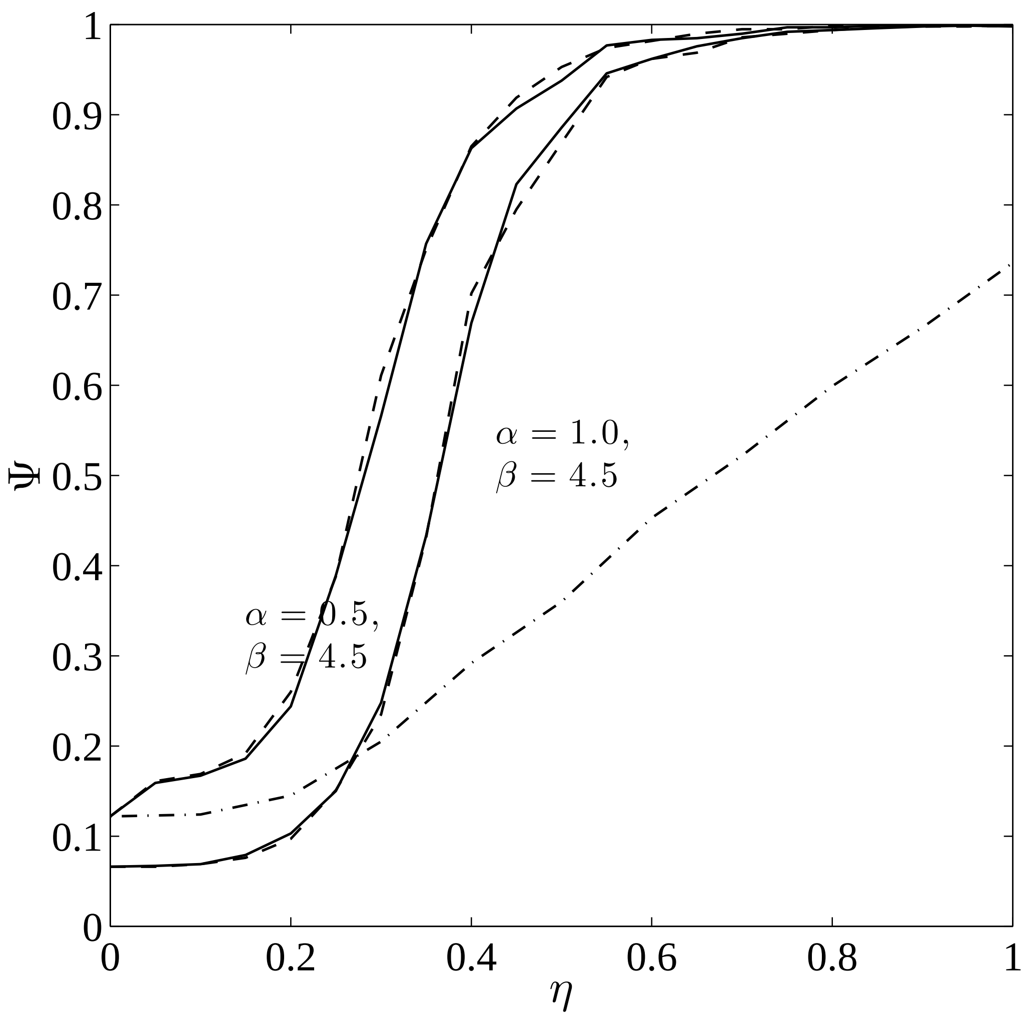

Fig. 3. Mapping function $\Psi(\eta, \beta, \alpha)$ with $\alpha = 1.0, 0.5$, at $E_b/N_0 = 6$dB and $\beta = 4.5$. Dashed lines represent the density evolution with the $(5,7)_8$ convolutional code and solid lines the approximation for data and activity detection. The dash-dotted line is classical Gaussian approximation.

Fig. 4 confirms the results of Corollary 4.4 for an activity rate $\alpha = 0.5$. The curves are essentially equal (up to numerical error) and only differ in the point $\eta^0 = 0$, which is not in the domain of the result. The scaling of the system load cannot reproduce the value at the very first iteration since the detection is done as if the system was uncoded. In fact, it is easy to see that the right limit of the scaling curve when $\eta^{(\ell-1)} \to 0$ does not coincide with the value at $\eta^{(\ell-1)} = 0$. The right limit is the fixed-point equation of a data detector with scaled system load $\alpha\beta$:

$$\eta^{(0)} = \frac{1}{1 + \alpha\beta\gamma \left(1 - \int \frac{e^{\frac{-y^2}{2}}}{\sqrt{2\pi}} \tanh\left(\eta^{(0)}\gamma - \sqrt{\eta^{(0)}\gamma} y\right) \mathrm{d}y\right)} \tag{20}$$

whereas the point $\Psi(0)$ is given by the user-and-data detection curve with the prior probabilities $\{\alpha/2, 1-\alpha, \alpha/2\}$:

$$\eta^{(0)} = \frac{1}{1 + \beta\gamma \left(\alpha - \int \frac{e^{\frac{-y^2}{2}}}{\sqrt{2\pi}} \frac{\alpha^2 \sinh(\eta^{(0)}\gamma - y\sqrt{\eta^{(0)}\gamma})}{\alpha \cosh(\eta^0\gamma - y\sqrt{\eta^0\gamma}) + (1-\alpha) e^{\eta^{(0)}\frac{\gamma}{2}}} \mathrm{d}y\right)} \tag{21}$$

which in general yield different solutions.

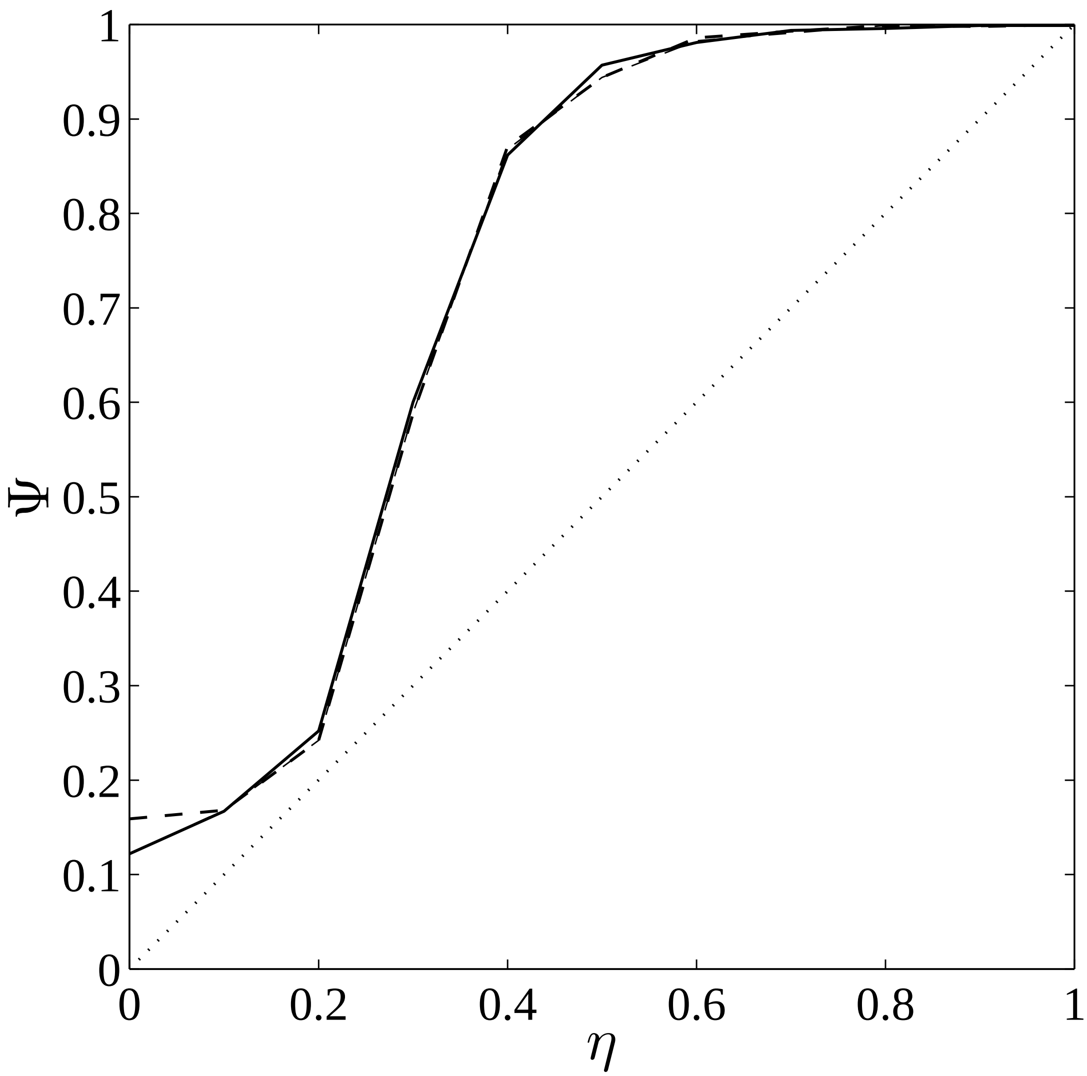

Fig. 4. Mapping function $\Psi(\eta, \beta, \alpha)$ with $\alpha = 0.5$, at $E_b/N_0 = 6$dB and $\beta = 4.5$. Solid lines represent density evolution for the $(5,7)_8$ convolutional code. Dash-dotted lines represent the approximation for data and activity detection under the same parameters, and the dashed curve represents the approximation with $\alpha = 1.0$ and $\beta' = 2.25$.

VI. Conclusions

Based on density evolution, we have characterized the large-system behavior of iterative multiuser joint decoding when the number of active users is unknown. In particular, we have characterized the fixed-point equations that yield the multiuser efficiency via the replica method. We have shown that under the assumptions of density evolution, the system effectively performs perfect activity detection and is hence equivalent to a system where the number of users is fixed and known, but with a scaled system load. We have also discussed the corresponding Gaussian approximations and we have verified that these approximations give very accurate characterizations of the overall behavior of the iterative multiuser joint decoder.

Appendix I
Proof of proposition 4.1

The block error probability P_e is given by the product of $L/2+1$ errors in a single detection when no data is transmitted. This is given by the expression

$$P_e = (2Q(\sqrt{\eta\gamma}/2))^{L/2+1}$$

where $Q(.)$ is the Gaussian tail function that can be upper-bounded in the following form. The success probability is then $P_s = 1 - P_e$.

Appendix II
Proof of claim 4.3

The proof lies on the so-called replica method, which is a common tool in statistical physics and has been proved to be a powerful technique in detection analysis. We mainly follow the derivation of this method in [10], which generalizes the pioneering study in [9]. In fact, the iterative decoding framework described above requires a generalization of classic uncoded detection to the case of arbitrary and unequal symbol prior probabilities, under the assumption that in the large-system limit, the empirical distribution of these priors converges almost everywhere to some deterministic function (concentration). The proof also extends the results for log-ratio prior probabilities in [5] to the case of arbitrary extrinsic message probabilities (p_{ext}), whose distribution is in turn governed by a Bernoulli variable x_α with mean equal to the activity rate. In other words, we analyze the more general case where extrinsic probability distributions are subjected to the presence of active users.

We start by analyzing an optimal generic multiuser detector. The receiver postulates an AWGN channel with noise variance σ and prior probability p_X, whereas the true noise variance is $\sigma_0^2 = 1$ and the prior probability is p_{X_0}, without loss of generalization. The replica method consists of adding n input symbols $X_1, \ldots, X_n$ and corresponding postulated channels to the true one, whose input is X_0.

By applying *Varadhan's lemma* and assuming *replica symmetry* among the solutions of the resulting optimization problem, the free energy can be expressed as

$$\begin{aligned}\mathcal{F} &= \lim_{n\to 0} \frac{\partial}{\partial n}\left(\inf_{\{c,d,f,g\}} \sup_{\{r,p,m,q\}} H(c,d,f,g,r,p,m,q)\right) \\ &= \lim_{n\to 0} \frac{\partial}{\partial n}\left(\inf_{\{c,d,f,g\}} \sup_{\{r,p,m,q\}} \left\{\beta^{-1} G^n(r,p,m,q) - I^n(c,d,f,g)\right\}\right) \qquad (22)\end{aligned}$$

where

$$G^n(r,p,m,q) = \frac{1}{2}\log\frac{(1+\frac{\beta}{\sigma^2}(p-q))^{1-n}}{1+\frac{\beta}{\sigma^2}(p-q)+\frac{n}{\sigma^2}(1+\beta(r-2m+q))} - \frac{n}{2}\log(2\pi\sigma^2) \qquad (23)$$

and

$$I^n(c,d,f,g) = rc + npg + 2nmd + n(n-1)qf - \lim_{K\to\infty}\frac{1}{K}\sum_{k=1}^{K}\log\Lambda_k^n(c,d,g,f) \tag{24}$$

is the rate function computed by the *Gärtner-Ellis* theorem, where $\Lambda_k^n(c,d,g,f)$ is the moment generating function for user k of the random vector $\{X_iX_j : i = 0,\ \dots, n, 0 \le j \le i\}$, generated by the two-term product of all replicas. In fact, note that it can be developed as:

$$\Lambda_k^n(c,d,g,f) = \mathbb{E}_{\boldsymbol{X}}\left[\exp\left(\gamma_k \boldsymbol{X}^T\boldsymbol{\mathcal{Q}}\boldsymbol{X}\right)\right] \tag{25}$$

$$= \mathbb{E}_{\boldsymbol{X}}\left[\exp\left[\gamma_k\left(2d\sum_{i=1}^{n}X_0X_i + 2f\sum_{1\le i<j\le n}X_iX_j + cX_0^2 + g\sum_{i=1}^{n}X_i^2\right)\right]\right] \tag{26}$$

where $\boldsymbol{\mathcal{Q}}$ is the matrix of parameters and the replicas $\boldsymbol{X} = (X_0,\dots,X_n)$ are independent but in general have different prior probabilities.

The overall computation of the free-energy is equivalent to a simple derivation of H over the symmetric replicas at $n = 0$:

$$\lim_{n\to 0}\frac{\partial H}{\partial(.)}$$

Hence, we immediately obtain:

$$\lim_{n\to 0}\frac{\partial H}{\partial r} = 0 \quad\Rightarrow\quad c = 0 \tag{27}$$

$$\lim_{n\to 0}\frac{\partial H}{\partial m} = 0 \quad\Rightarrow\quad d = \frac{1}{2[\sigma^2+\beta(p-q)]} \tag{28}$$

$$\lim_{n\to 0}\frac{\partial H}{\partial q} = 0 \quad\Rightarrow\quad f = \frac{1+\beta(r-2m+q)}{2(\sigma^2+\beta(p-q))} \tag{29}$$

$$\lim_{n\to 0}\frac{\partial H}{\partial p} = 0 \quad\Rightarrow\quad g = f - d \tag{30}$$

The rest of parameters are found by derivation of the moment generating function (26) with respect to c, d, f, g.

$$\lim_{n\to 0}\frac{\partial H}{\partial(.)} = \lim_{n\to 0}\lim_{K\to\infty}\frac{1}{K}\sum_{k=1}^{K}\frac{\partial\left(\log\Lambda_k^n(c,d,g,f)\right)}{\partial(.)} = 0 \tag{31}$$

By applying the law of large numbers to (31), we have

$$\lim_{n\to 0}\frac{\partial H}{\partial c} = 0 \Rightarrow r = \lim_{n\to 0}\mathbb{E}_{x_\alpha,\boldsymbol{p}_{\text{ext}},\boldsymbol{X},\gamma}\left[\frac{X_0^2\gamma\exp\left(\boldsymbol{X}^T\boldsymbol{\mathcal{Q}}\boldsymbol{X}\right)}{\Lambda^n(c,d,g,f)}\right]$$

$$\lim_{n\to 0}\frac{\partial H}{\partial g} = 0 \Rightarrow np = \lim_{n\to 0}\mathbb{E}_{x_\alpha,\boldsymbol{p}_{\text{ext}},\boldsymbol{X},\gamma}\left[\frac{\sum_{i=1}^{n}X_i^2\exp\left(\boldsymbol{X}^T\boldsymbol{\mathcal{Q}}\boldsymbol{X}\right)}{\Lambda^n(c,d,g,f)}\right]$$

$$\lim_{n\to 0}\frac{\partial H}{\partial d} = 0 \Rightarrow 2nm = \lim_{n\to 0}\mathbb{E}_{\boldsymbol{p}_\alpha,\boldsymbol{p}_{\text{ext}},\boldsymbol{X},\gamma}\left[\frac{2\sum_{i=1}^{n}X_0X_i\exp\left(\boldsymbol{X}^T\boldsymbol{\mathcal{Q}}\boldsymbol{X}\right)}{\Lambda^n(c,d,g,f)}\right]$$

$$\lim_{n\to 0}\frac{\partial H}{\partial f} = 0 \Rightarrow n(n-1)q = \lim_{n\to 0}\mathbb{E}_{x_\alpha,\boldsymbol{p}_{\text{ext}},\boldsymbol{X},\gamma}\left[\frac{2\sum_{1\le i<j\le n}X_iX_j\exp\left(\boldsymbol{X}^T\boldsymbol{\mathcal{Q}}\boldsymbol{X}\right)}{\Lambda^n(c,d,g,f)}\right]$$

where $\Lambda^n(c,d,g,f) = \mathbb{E}_{\boldsymbol{X}}\left[\exp\left(\gamma\boldsymbol{X}^T\boldsymbol{\mathcal{Q}}\boldsymbol{X}\right)\right]$ and $\gamma \sim \gamma_k$. We can further develop the above equations by using the unit area property of the Gaussian density

$$e^{t^2} = \sqrt{\frac{\eta}{2\pi}}\int\exp\left[-\frac{\eta}{2}z^2 + \sqrt{2\eta}tz\right]\mathrm{d}z, \quad \forall t,\eta \tag{32}$$

which yields

$$\Lambda^n(c,d,g,f)=\mathbb{E}_{\boldsymbol{X}}\left[\sqrt{\frac{d^2}{f\pi}}\int\exp\left[-\frac{d^2}{f}(z-\sqrt{\gamma}X_0)^2+c\gamma X_0\right]\prod_{i=1}^{n}\mathbb{E}_{X_i}[\exp[2d\sqrt{\gamma}X_iz+(g-f)\gamma X_i^2]|\gamma]\mathrm{d}z\right] \tag{33}$$

Notice that $c=0$, and $d=f-g$, and (33) can be written as:

$$\Lambda^n(c,d,g,f)=\mathbb{E}_{\boldsymbol{X}}\left[\sqrt{\frac{\eta}{2\pi}}\int\exp\left[-\frac{\eta}{2}(z-\sqrt{\gamma}X_0)^2\right]\prod_{i=1}^{n}\mathbb{E}_{X_i}\left[\exp\left[-\frac{\xi}{2}-\frac{\xi}{2}(z-\sqrt{\gamma}X_i)\right]|\gamma\right]\mathrm{d}z\right] \tag{34}$$

where $\eta=2d^2/f$ and $\xi=2d$ are the multiuser efficiency of the original and postulated channel respectively. Then, it is easy to see that:

$$\lim_{n\to 0}\Lambda^n(c,d,g,f)=1 \tag{35}$$

The parameter r can therefore be computed straightforwardly

$$\begin{aligned}\lim_{n\to 0}\frac{\partial H}{\partial c}=0\Rightarrow r&=\lim_{n\to 0}\mathbb{E}_{x_\alpha,\boldsymbol{p}_{\text{ext}},\boldsymbol{X},\gamma}\left[\frac{X_0^2\gamma\exp\left(\boldsymbol{X}^T\boldsymbol{\mathcal{Q}}\boldsymbol{X}\right)}{\Lambda^n(c,d,g,f)}\right]\\&=\mathbb{E}_{x_\alpha,\boldsymbol{p}_{\text{ext}},\boldsymbol{X},\gamma}[\gamma X_0^2]\end{aligned} \tag{36}$$

Note that for p, we have:

$$\begin{aligned}\lim_{n\to 0}\frac{\partial H}{\partial g}=0\Rightarrow np&=\lim_{n\to 0}\mathbb{E}_{x_\alpha,\boldsymbol{p}_{\text{ext}},\boldsymbol{X},\gamma}\left[\frac{\sum_{i=1}^{n}X_i^2\exp\left(\boldsymbol{X}^T\boldsymbol{\mathcal{Q}}\boldsymbol{X}\right)}{\Lambda^n(c,d,g,f)}\right]\\&=\mathbb{E}_{x_\alpha,\boldsymbol{p}_{\text{ext}},\gamma}\left[\gamma\sum_{i=1}^{n}(\Pr(X_i=1)-\Pr(X_i=-1))|\boldsymbol{X}\right]\\&=n\left(\sum_{x_\alpha}x_\alpha\mathbb{E}_{\boldsymbol{p}_{\text{ext}}|x_\alpha,\gamma}[\gamma\Pr(X=1)|\boldsymbol{X},x_\alpha]-\mathbb{E}_{\boldsymbol{p}_{\text{ext}}|x_\alpha,\gamma}[\gamma\Pr(X=-1)|\boldsymbol{X},x_\alpha]\right)\end{aligned}$$

where $\boldsymbol{p}_{\text{ext}}|x_\alpha=\{\Pr(X=-1),\Pr(X=0),\Pr(X=1)|x_\alpha\}$ are distributed as $\{\Pr(X_i=-1),\Pr(X_i=0),\Pr(X_i=1)|x_\alpha\}$, $\forall i\in\{1,\ldots,n\}$. Then:

$$p=\lim_{n\to 0}\mathbb{E}_{x_\alpha,\boldsymbol{p}_{\text{ext}},\boldsymbol{X},\gamma}[\gamma X^2] \tag{37}$$

Similarly, we have:

$$\begin{aligned}&\lim_{n\to 0}\frac{\partial H}{\partial d}=0\Rightarrow 2nm=\lim_{n\to 0}\mathbb{E}_{x_\alpha,\boldsymbol{p}_{\text{ext}},\boldsymbol{X},\gamma}\left[\frac{2\sum_{i=1}^{n}X_0X_i\exp\left(\boldsymbol{X}^T\boldsymbol{\mathcal{Q}}\boldsymbol{X}\right)}{\Lambda^n(c,d,g,f)}\right]\\&=\mathbb{E}_{x_\alpha,\boldsymbol{p}_{\text{ext}},\boldsymbol{X},\gamma}\left[\gamma\sqrt{\frac{\eta}{2\pi}}\int\exp\left[-\frac{\eta}{2}(z-\sqrt{\gamma}X_0)^2\right]2\sum_{i=1}^{n}X_0X_i\right]\\&=\mathbb{E}_{x_\alpha,\boldsymbol{p}_{\text{ext}},\boldsymbol{X},\gamma}\left[2\gamma X_0\sum_{i=1}^{n}\sqrt{\frac{\eta}{2\pi}}\int\exp\left[-\frac{\eta}{2}(z-\sqrt{\gamma}X_0)^2\right]\frac{X_i\sqrt{\frac{\xi}{2\pi}}\int\exp\left[-\frac{\xi}{2}(z-\sqrt{\gamma}X_i)\right]}{\mathbb{E}_{X_i}[\sqrt{\frac{\xi}{2\pi}}\int\exp\left[-\frac{\xi}{2}(z-\sqrt{\gamma}X_i)\right]|\gamma]}\mathrm{d}z\right]\\&=\mathbb{E}_{x_\alpha,\boldsymbol{p}_{\text{ext}},\boldsymbol{X},\gamma}\left[2\gamma X_0\sum_{i=1}^{n}\sqrt{\frac{\eta}{2\pi}}\int\exp\left[-\frac{\eta}{2}(z-\sqrt{\gamma}X_0)^2\right]\hat{X}_i\mathrm{d}z\right]\end{aligned}$$

where $f(z|X_i) = \sqrt{\frac{\xi}{2\pi}} \exp\left[-\frac{\xi}{2}(z - \sqrt{\gamma}X_i)\right]$ is an auxiliary Gaussian channel and $\hat{X}_i$ is the posterior mean estimator of the replica X_i. Notice that the above expression can be expressed as an expectation over the variables $\boldsymbol{X}, \gamma, Z$:

$$\begin{aligned} 2nm &= 2\mathbb{E}_{x_\alpha, \boldsymbol{p}_{\text{ext}}, \boldsymbol{z}, X_0, \gamma}\left[\gamma X_0 \sum_{i=1}^{n} \hat{X}_i\right] = 2\mathbb{E}_{x_\alpha, \boldsymbol{p}_{\text{ext}}, \boldsymbol{z}}\left[\sum_{i=1}^{n} \hat{X}_i\right] \mathbb{E}_{x_\alpha, \boldsymbol{p}_{\text{ext}}, \boldsymbol{z}, X_0, \gamma}\left[\gamma X_0\right] \\ &= 2n\mathbb{E}_{x_\alpha, \boldsymbol{p}_{\text{ext}}, \boldsymbol{z}}\left[\hat{X}\right] \mathbb{E}_{\boldsymbol{p}_{\text{ext}}, \boldsymbol{z}, X_0, \gamma}\left[\gamma X_0\right] = 2n\mathbb{E}_{x_\alpha, \boldsymbol{p}_{\text{ext}}, \boldsymbol{z}, X_0, \gamma}\left[\gamma X_0 \hat{X}\right] \\ \Rightarrow m &= \mathbb{E}_{x_\alpha, \boldsymbol{p}_{\text{ext}}, \boldsymbol{z}, X_0, \gamma}\left[\gamma X_0 \hat{X}\right] \end{aligned}$$

where it is used that the expectation of all $\hat{X}_i$ over $\boldsymbol{p}_{\text{ext}}|x_\alpha$ yields the same result. In fact, the random variable $\hat{X}|x_\alpha$ has the same distribution of $\hat{X}_i|x_\alpha$, $\forall i \in \{1, \ldots, n\}$. Similarly,

$$q = \mathbb{E}_{x_\alpha, \boldsymbol{p}_{\text{ext}}, \boldsymbol{z}, \boldsymbol{X}, \gamma}\left[\gamma \hat{X}^2\right] \tag{38}$$

By simple combination between the replicas, it is easy to see that:

$$\begin{aligned} r - 2m + q = &= \mathbb{E}_{x_\alpha, \boldsymbol{p}_{\text{ext}}, \boldsymbol{z}, \boldsymbol{X}, \gamma}\left[\gamma\left(X_0 - \hat{X}\right)^2\right] \\ p - q &= \mathbb{E}_{x_\alpha, \boldsymbol{p}_{\text{ext}}, \boldsymbol{z}, \boldsymbol{X}, \gamma}\left[\gamma\left(X - \hat{X}\right)^2\right] \end{aligned}$$

which in turn leads to the fixed-point equations

$$\begin{aligned} \eta^{-1} &= 1 + \beta\mathbb{E}_{x_\alpha, \boldsymbol{p}_{\text{ext}}, \boldsymbol{z}, \boldsymbol{X}, \gamma}\left[\gamma\left(X_0 - \hat{X}\right)^2\right] \\ \xi^{-1} &= \sigma^2 + \beta\mathbb{E}_{x_\alpha, \boldsymbol{p}_{\text{ext}}, \boldsymbol{z}, \boldsymbol{X}, \gamma}\left[\gamma\left(X - \hat{X}\right)^2\right] \end{aligned}$$

using (27)-(30) and the definition of (η, ξ).

For the case of interest here, i.e., individually optimum detection, the postulated noise variance σ^2 coincides with the true variance $\sigma_0 = 1$ so that the replica solution $\eta = \xi$ is chosen, and the fixed-point equation is reduced to:

$$\eta^{-1} = 1 + \beta\mathbb{E}_{x_\alpha, \boldsymbol{p}_{\text{ext}}, \boldsymbol{z}, \boldsymbol{X}, \gamma}\left[\gamma\left(X - \hat{X}\right)^2\right] \tag{39}$$

Since $\boldsymbol{p}_{\text{ext}}$ depends on the state of the channel in the previous iteration, we can express the result recursively in the following manner:

$$\eta^{(\ell)} = \left(1 + \beta\mathbb{E}_{x_\alpha, \boldsymbol{p}_{\text{ext}}, \boldsymbol{z}, \boldsymbol{X}, \gamma}\left[\gamma\left(X - \hat{X}\right)^2\right]\right)^{-1} \tag{40}$$

where the MMSE estimate can be expressed as $\hat{X} = \hat{X}(\eta^{(\ell-1)}, \eta^{(\ell)}, \gamma)$.

APPENDIX III
PROOF OF COROLLARY 4.4

As seen in proposition 4.1, the extrinsic probabilities converge with probability 1 to:

$$(\boldsymbol{p}_{ext}|x_\alpha = 0) = (p_{(-1)}, p_0, p_1) \to (0, 1, 0) \tag{41}$$

regardless of the positive value of SNR. Hence, the fixed-point equation can be simplified by noticing that:

$$\mathbb{E}_{x_\alpha,\boldsymbol{p}_{\text{ext}},\boldsymbol{z},\boldsymbol{X},\gamma}\left[\gamma\left(X-\hat{X}\right)^2\right] = \alpha\mathbb{E}_{\boldsymbol{p}_{\text{ext}},\boldsymbol{z},\boldsymbol{X},\gamma|x_\alpha=1}\left[\gamma\left(X-\hat{X}\right)^2\right] + (1-\alpha)\mathbb{E}_{\boldsymbol{p}_{\text{ext}},\boldsymbol{z},\boldsymbol{X},\gamma|x_\alpha=0}\left[\gamma\left(X-\hat{X}\right)^2\right] \tag{42}$$

where the last term tends to zero due to the deterministic probabilities (41). Assuming that the SNR is constant among users, we finally have:

$$\begin{aligned}\eta^{(\ell)} &= \left(1+\beta\alpha\gamma\mathbb{E}_{(\boldsymbol{p}_{ext}|x_\alpha=1),z,\boldsymbol{X}}\left[\gamma\left(X-\hat{X}\right)^2\right]\right)^{-1} \\ &= \left(1+\beta\alpha\gamma\left(1-\mathbb{E}_{\boldsymbol{p}_{ext}|x_\alpha=1,z,\boldsymbol{X}}\left[\gamma\hat{X}^2\right]\right)\right)^{-1}\end{aligned} \tag{43}$$

where $\hat{X}=\hat{X}(\eta^{(\ell-1)},\eta^{(\ell)},\gamma)$.

Appendix IV
Proof of Corollary 4.5

We use here the aforementioned Gaussian approximation of the probability messages, that states that when there is an active user ($x_\alpha=1$, with probability α), the virtual channel at the SISO decoder can be approximated by the distribution $\delta\sim\mathcal{N}(0,1/(\mu(\gamma\eta^{\ell-1})))$. Hence, the extrinsic probabilities can be computed as APP's of this virtual channel:

$$(\boldsymbol{p}_{ext}|x_\alpha=1)=(p_{(-1)},p_0,p_1)=\frac{1}{Z(y)\sqrt{2\pi}}\left(\frac{\alpha}{2}e^{\frac{(y-\sqrt{\mu(\eta\gamma)})^2}{2}},(1-\alpha)e^{-\frac{y^2}{2}},\frac{\alpha}{2}e^{-\frac{(y+\sqrt{\mu(\eta\gamma)})^2}{2}}\right) \tag{44}$$

where $Z(y)$ is the p.d.f. of the variable y.

Further development of (15) yields:

$$\begin{aligned}\mathbb{E}_{y,z,X}[\hat{X}^2] &= \mathbb{E}_{y,X}\left[\int\frac{\left(\frac{1}{2\pi}\left[e^{-\frac{1}{2}\left((z-\sqrt{\eta\gamma})^2-(y-\sqrt{\mu(\eta\gamma)})^2\right)}-e^{-\frac{1}{2}\left((z+\sqrt{\eta\gamma})^2-(y+\sqrt{\mu(\eta\gamma)})^2\right)}\right]\right)^2}{\frac{1}{2\pi}\left(e^{-\frac{1}{2}\left((z-\sqrt{\eta\gamma})^2-(y-\sqrt{\mu(\eta\gamma)})^2\right)}+e^{-\frac{1}{2}\left((z+\sqrt{\eta\gamma})^2-(y+\sqrt{\mu(\eta\gamma)})^2\right)}\right)}\right] \\ &= \int_{\mathbb{R}^2}\frac{1}{2\pi}e^{-\frac{(y^2+z^2)}{2}}\tanh\left(\eta^{(\ell)}\gamma+\mu(\eta^{(\ell-1)}\gamma)-\sqrt{\eta^{(\ell)}\gamma}y-\sqrt{\mu(\eta^{(\ell-1)}\gamma)}z\right)\mathrm{d}y\mathrm{d}z\end{aligned}$$

which is the claimed result.

Appendix V
Proof of Proposition 4.6

The MMSE for the iterative multiuser detector with Gaussian approximation can be written in the following form:

$$\text{MMSE}=1-\frac{1}{2\pi}\int_{\mathbb{R}^2}e^{-\frac{y^2+z^2}{2}}\tanh\left(\mu+\gamma-\sqrt{\mu}z-\sqrt{\gamma}y\right)dydz$$

Here, we make the change of variable $y'=-y+\sqrt{\gamma}+\frac{\mu-\sqrt{\mu}z}{\sqrt{\gamma}}$ and we obtain:

$$\text{MMSE}=1-\frac{1}{2\pi}\int e^{-\frac{z^2}{2}}\int e^{-\frac{\left(y'-\sqrt{\gamma}-\frac{\mu-\sqrt{\mu}z}{\sqrt{\gamma}}\right)^2}{2}}\tanh\left(\sqrt{\gamma}y'\right)dy'dz$$

We use now the asymptotic expansion $\tanh(z) = \mathrm{sgn}(z)\left(1 + \sum_{\ell=1}^{\infty}(-1)^{\ell} e^{-2\ell|z|}\right)$ for large z. Hence in the case of the argument $z = \gamma y'$, the expression turns out to be:

$$\lim_{\gamma\to\infty} \mathrm{MMSE} = 1 - \frac{1}{\sqrt{2\pi}} \int e^{-\frac{z^2}{2}} \left(\int_{-\infty}^{0} -e^{-\frac{\left(y'-\sqrt{\gamma}-\frac{\mu-\sqrt{\mu}z}{\sqrt{\gamma}}\right)^2}{2}} dy' + \int_{0}^{\infty} e^{-\frac{\left(y'-\sqrt{\gamma}-\frac{\mu-\sqrt{\mu}z}{\sqrt{\gamma}}\right)^2}{2}} dy' \right) dz$$

$$= 1 - \frac{1}{\sqrt{2\pi}} \int e^{-\frac{z^2}{2}} \left(\frac{1}{\sqrt{2\pi}} \int_{-\infty}^{0} -e^{-\frac{\left(y'-\sqrt{\gamma}-\frac{\mu-\sqrt{\mu}z}{\sqrt{\gamma}}\right)^2}{2}} dy + \frac{1}{\sqrt{2\pi}} \int_{0}^{\infty} e^{-\frac{\left(y'-\sqrt{\gamma}-\frac{\mu-\sqrt{\mu}z}{\sqrt{\gamma}}\right)^2}{2}} dy' \right) dz$$

We make the change of variables $t = y' - \sqrt{\gamma} - \frac{\mu-\sqrt{\mu}z}{\sqrt{\gamma}}$ and $t' = -\left(y' - \sqrt{\gamma} - \frac{\mu-\sqrt{\mu}z}{\sqrt{\gamma}}\right)$, and using the Q function, and the relationship $Q(-x) = 1 - Q(x)$ we obtain:

$$\lim_{\gamma\to\infty} \mathrm{MMSE} = \frac{1}{\sqrt{2\pi}} \int e^{-\frac{z^2}{2}} 2Q\left(\sqrt{\gamma} + \frac{\mu-\sqrt{\mu}z}{\sqrt{\gamma}}\right) dz$$

We use now the asymptotic expansion of the Q function:

$$Q(x) = \frac{e^{-x^2/2}}{\sqrt{2\pi}x}\left(1 + \sum_{\ell=1}^{\infty}(-1)^{\ell}\frac{\prod_{q=1}^{\ell}(2q-1)}{x^{2\ell}}\right) \tag{45}$$

and express the MMSE as:

$$\lim_{\gamma\to\infty} \mathrm{MMSE} = \frac{2}{2\pi} \int e^{-\frac{z^2}{2}} \frac{e^{-\frac{\left(\sqrt{\gamma}+\frac{\mu-\sqrt{\mu}z}{\sqrt{\gamma}}\right)^2}{2}}}{\sqrt{\gamma} + \frac{\mu-\sqrt{\mu}z}{\sqrt{\gamma}}} dz$$

$$\lim_{\gamma\to\infty} \mathrm{MMSE} = \frac{2e^{-\frac{\gamma}{2}-\mu-\frac{\mu^2}{2\gamma}}}{2\pi} \int e^{-\frac{z^2}{2}} \frac{e^{(1+\frac{\mu}{\sqrt{\gamma}})\sqrt{\mu}z - \frac{\mu z^2}{2\gamma}}}{\sqrt{\gamma} + \frac{\mu-\sqrt{\mu}z}{\sqrt{\gamma}}} dz$$

After some manipulation we have:

$$\lim_{\gamma\to\infty} \mathrm{MMSE} = \frac{2e^{-\frac{\gamma}{2}-\mu-\frac{\mu^2}{2\gamma}}}{2\pi} \int \frac{e^{-\frac{1}{2}\left((\frac{\mu}{\gamma}+1)z^2 - 2(1+\frac{\mu}{\sqrt{\gamma}})\sqrt{\mu}z\right)}}{\sqrt{\gamma} + \frac{\mu-\sqrt{\mu}z}{\sqrt{\gamma}}} dz$$

For convenience, we convert the expression into the following one:

$$\lim_{\gamma\to\infty} \mathrm{MMSE} = \frac{2e^{-\frac{\gamma}{2}-\mu-\frac{\mu^2}{2\gamma}+\frac{(1+\frac{\mu}{\sqrt{\gamma}})\sqrt{\mu}}{2(1+\frac{\mu}{\gamma})}}}{2\pi} \int \frac{e^{-\frac{1}{2}\left(\left(1+\frac{\mu}{\gamma}\right)z - \frac{(1+\frac{\mu}{\sqrt{\gamma}})\sqrt{\mu}}{1+\frac{\mu}{\gamma}}\right)^2}}{\sqrt{\gamma} + \frac{\mu-\sqrt{\mu}z}{\sqrt{\gamma}}} dz$$

We make now the change of variable $t = (1 + \frac{\mu}{\gamma})z - \frac{(1+\frac{\mu}{\sqrt{\gamma}})\sqrt{\mu}}{1+\frac{\mu}{\gamma}}$, and then:

$$\lim_{\gamma\to\infty} \mathrm{MMSE} = \frac{2e^{-\frac{\gamma}{2}-\mu-\frac{\mu^2}{2\gamma}+\frac{(1+\frac{\mu}{\sqrt{\gamma}})\sqrt{\mu}}{2(1+\frac{\mu}{\gamma})}}}{2\pi} \int \frac{e^{-\frac{t^2}{2}}}{\sqrt{\gamma} + \frac{\mu-\sqrt{\mu}\left(\frac{t}{\left(1+\frac{\mu}{\gamma}\right)} + \frac{(1+\frac{\mu}{\sqrt{\gamma}})\sqrt{\mu}}{\left(1+\frac{\mu}{\gamma}\right)^2}\right)}{\sqrt{\gamma}}} dt$$

Using the Saddle-point approximation of the integral and taking the value of the integrand in $t = 0$ for large SNR, we find that:

$$\lim_{\gamma\to\infty} \text{MMSE} = \frac{2e^{-\frac{\gamma}{2}-\mu-\frac{\mu^2}{2\gamma}+\frac{(1+\frac{\mu}{\sqrt{\gamma}})\sqrt{\mu}}{2(1+\frac{\mu}{\gamma})}}}{\sqrt{2\pi}\left(\sqrt{\gamma}+\frac{\mu-\sqrt{\mu}\frac{(1+\frac{\mu}{\sqrt{\gamma}})\sqrt{\mu}}{\left(1+\frac{\mu}{\gamma}\right)^2}}{\sqrt{\gamma}}\right)}$$

Finally,

$$\lim_{\gamma\to\infty} \text{MMSE} = \sqrt{\frac{2}{\pi}}\frac{e^{-\frac{\gamma}{2}-\mu-\frac{\kappa_1^2}{2}+\frac{(1+\kappa_1)\sqrt{\mu}}{2(1+\kappa_2)}}}{\sqrt{\gamma}+\kappa_1\left(1-\frac{(1+\kappa_1)}{(1+\kappa_2)^2}\right)}$$

where $\kappa_1 = \frac{\mu(\eta\gamma)}{\sqrt{\eta\gamma}}$ and $\kappa_2 = \frac{\mu(\eta\gamma)}{\eta\gamma}$.

References

[1] A. Grant and C. Schlegel, *Coordinated multiuser communications*, Springer, New York, 2006.

[2] M. Reed, C. Schlegel, P. Alexander, and J. Asentorfer, "Iterative multiuser detection for CDMA with FEC: Near single-user performance," *IEEE Trans. Commun.*, vol. 46, pp. 1693–1699, Dec. 1998.

[3] X. Wang and V. Poor, "Iterative (turbo) soft interference cancellation and decoding for coded CDMA," *IEEE Trans. Commun.*, vol. 47, pp. 1047–1061, Jul. 1999.

[4] J. Boutros and G. Caire, "Iterative multiuser joint decoding," *IEEE Trans. Inf. Theory*, vol. 48, no. 7, pp. 1772–1793, Jul. 2002.

[5] G.Caire, R. R. Müller, and T. Tanaka, "Iterative multiuser joint decoding: Optimal power allocation and low-complexity implementation," *IEEE Trans. Inf. Theory*, vol. 50, no. 9, pp. 1950–1973, Sep. 2004.

[6] F. Kschischang, B. Frey, and H.-A. Loeliger, "Factor graphs and the sum-product algorithm," *IEEE Trans. Inf. Theory*, vol. 47, no. 2, pp. 498–519, Feb. 2001.

[7] T. Richardson and R.L. Urbanke, *Modern coding theory*, Cambridge University Press, New York, 2008.

[8] D. Tse and S. Hanly, "Linear multiuser receivers: effective interference, effective bandwidth, and user capacity," *IEEE Trans. Inf. Theory*, vol. 45, no. 2, pp. 641–657, March 1999.

[9] T. Tanaka, "A statistical-mechanics approach to large-system analysis of CDMA multiuser detectors," *IEEE Trans. Inf. Theory*, vol. 48, no. 11, pp. 2888–2910, Nov. 2002.

[10] D. Guo and S. Verdú, "Randomly spread CDMA: Asymptotics via statistical physics," *IEEE Trans. Inform. Theory*, vol. 51, no. 6, pp. 1983–2007, June 2005.

[11] R. R. Müller, "Channel capacity and minimum probability of error in large dual antenna array systems with binary modulation," *IEEE Trans. Signal Processing*, vol. 51, no. 11, pp. 2821–2828, November 2003.

[12] E. Biglieri and M. Lops, "Multiuser detection in a dynamic environment- Part I: User identification and data detection," *IEEE Trans. Info.. Theory*, vol. 53, no. 9, pp. 3158–3170, September 2007.

[13] D. Guo and T. Tanaka, "Generic multiuser detection and statistical physics," in *Advances in Multiuser Design*. 2008, M. L. Honig Ed. John Wiley & Sons.

[14] L. Bahl, J. Cocke, F. Jelinek, and J. Raviv, "Optimal decoding of linear codes for minimizing symbol error rate," *Information Theory, IEEE Transactions on*, vol. 20, no. 2, pp. 284–287, Mar 1974.

[15] A. Tauste Campo, A. Guillén i Fàbregas, and E. Biglieri, "Large-system analysis of multiuser detection with an unknown number of users," Tech. Rep. CUED/F-INFENG/TR.601, Department of Engineering, University of Cambridge, May 2008, ISSN 0951-9211.